Original Article

http://dx.doi.org/10.3348/kjr.2012.13.5.572
pISSN 1229-6929 · eISSN 2005-8330
Korean J Radiol 2012;13(5):572-578

Korean Journal of Radiology
KJR

Anatomy of the Sinoatrial Nodal Branch in Korean Population: Imaging with MDCT

Yong Sub Song, MD, Whal Lee, MD, Eun-Ah Park, MD, Jin Wook Chung, MD, Jae Hyung Park, MD

All authors: Department of Radiology, Seoul National University College of Medicine, Seoul 110-744, Korea

Objective: To evaluate, on a retrospective basis, the anatomic characteristics of the arterial supply to the sinoatrial node (SAN) in the Korean population using an ECG-gated multi-detector CT (MDCT).

Materials and Methods: The electrocardiographic-gated MDCTs of 500 patients (258 men and 242 women; age range, 17-83 years; mean age, 58.6 ± 12.04 years) were analyzed retrospectively. In each case, the SAN artery (arteries) was named according to a special nomenclature with regard to origin, course, and termination.

Results: A total of 516 SAN arteries were visualized in 496 patients. The SAN was supplied by a single artery in 476 (96.4%) cases and by 2 arteries in 18 (3.6%) cases. The SAN originated from the right coronary artery in 265 (53.4%) cases and from the left circumflex in 213 (43%) cases.

Conclusion: This study can provide basic data on variations of the SAN artery in the Korean population.

Index terms: *Sinoatrial node; Sinoatrial nodal artery; SA node; ECG-gated MDCT; Korean population*

INTRODUCTION

Since the sinoatrial node (SAN) acts as a pace maker, ischemia of SAN due to iatrogenic occlusion or injury of SAN artery during surgery, coronary stent insertion or balloon inflation can cause arrhythmia such as atrial flutter or sick sinus syndrome (1, 2). Thus, the origin, course, and the number of SAN arteries are crucial information for the cardiologist and heart surgeon during surgery and catheter-related procedures. As the heart is one of the organs in which vascular variations are frequently observed (3-5), variable variations of SAN arteries have been reported in previous studies performed by anatomical dissection or catheter angiography (6-18). Recently, multi-detector row computed tomography (MDCT) has been used for evaluating anatomical variance of arteries (19, 20). Likewise, advances in electrocardiographic (ECG)-gated cardiac MDCT provides adequate temporal and spatial resolution for characterization of the smaller branches of epicardial coronary arteries. Several studies have evaluated SAN arterial variations using MDCT (21-24). However, the extent of the variations differs in frequency between studies. Ethnic differences between the study groups were suggested as a cause of these differences (8, 15-17, 23, 24). Thus, results of previous studies performed in specific ethnic groups may not be simply applied to another ethnic population. Correspondingly, types or frequencies of SAN arterial variations in the Korean population may be somewhat different from previously reported results.

Received December 24, 2011; accepted after revision March 26, 2012.
This study was partly supported by Leading Foreign Research Institute Recruitment Program through the National Research Foundation of Korea (NRF) funded by the Ministry of Education, Science and Technology (MEST) (0640-20100001).
Corresponding author: Whal Lee, MD, Department of Radiology, Seoul National University College of Medicine, 101 Daehak-ro, Jongno-gu, Seoul 110-744, Korea.
• Tel: (822) 2072-2584 • Fax: (822) 743-6385
• E-mail: whal.lee@gmail.com

Korean Journal of Radiology
KJR

Currently and to the best of our knowledge, there has been no systemic evaluation of the origin, course, and the number of the SAN artery in Korean population. Thus, the purpose of our study was to evaluate the anatomic characteristics of the arterial supply to the SAN in the Korean population using ECG-gated MDCT on a retrospective basis.

MATERIALS AND METHODS

Patient Population

Between June 2010 to September 2010, 643 patients, either self-referred because of a personal health concern or referred by a physician because of suspected coronary artery disease (CAD), underwent ECG-gated MDCT. Among them, we excluded 143 patients who turned out to have CAD because CAD can develop epicardial collateral vessels which may mislead the analysis of coronary variation (25, 26). After exclusion, 500 patients (258 men and 242 women; age range, 17-83 years; mean age, 58.62 ± 12.04 years) constituted our study population. There was no case with severe motion artifact leading to difficulty in evaluation of the coronary arterial path. The study protocol was confirmed and approved by the Institutional Review Board of Seoul National University Hospital, and informed consent was waived.

MDCT Protocol

All CT examinations were performed using a dual source CT scanner (Somatom Definition; Siemens Medical Solutions, Forchheim, Germany). Unless contraindicated, 100 mg of metoprolol (Betaloc; AstraZeneca, Yuhan, Seoul, Korea) was orally administered 1 hour prior to the examination to patients with a pre-scanning heart rate of at least 65 beats per minute. After establishing antecubital IV access in all patients, 80 mL of contrast media (Ultravist 370; Shering, Berlin, Germany) were injected, followed by 50 mL of an 8 : 2 mixture of normal saline and contrast medium at a flow rate of 4 mL/s with the use of a dual power injector (Stellant; Medrad, Indianola, PA, USA). The bolus triggering method was used to determine the beginning of CT acquisition by monitoring the signal density of the contrast medium in the mid-ascending aorta. The CT scan was started 8 seconds after a threshold trigger of 150 HU above baseline was reached.

Data acquisition was performed in the caudocranial direction with a detector collimation of 32 x 0.6 mm, a section collimation of 64 x 0.6 mm with a z-flying focal spot, a gantry rotation time of 330 ms and a tube voltage of 100 kVp. The pitch was automatically adapted to the heart rate: 0.20 (40 bpm), 0.26 (60 bpm), 0.32 (70 bpm), 0.37 (80 bpm), 0.43 (90 bpm) and 0.50 (100 bpm). Data sets were reconstructed with retrospective ECG-gating with a 0.6-0.8 mm slice thickness and 0.6-0.8 mm increments using a B26 soft-tissue reconstruction kernel. CT images are reconstructed at the best diastolic or systolic phase to evaluate the coronary arteries. Volume computed tomography does index provided by the CT machines varied from 23.46 to 55.18 mGy.

MDCT Imaging Analysis

One experienced observer reviewed the CT images. All CT datasets were transferred to a workstation installed with three-dimensional reconstruction software (Rapidia; Infinity, Seoul, Korea). Depending on the individual SAN arterial anatomy and image quality, different visualization techniques, such as multiplanar reformation, maximum intensity projection, and volume-rendering were used.

The SAN artery types were determined by using a classification system similar to the system used by Ortale et al. (17). According to this classification, each SAN artery was classified into one of following types: right or left (R or L), according to respective origin from the right coronary artery (RCA) or left circumflex (LCX); subtypes R1 or R2, according to its respective course medial to the right auricle or on the posterior surface of the right atrium (Fig. 1); or L1, L2 or L3, according to its respective course, medial, or posterior to the left auricle or, on the posterior surface of the left atrium (Fig. 2). Then, each type was subdivided according to the course of the terminal segment around the SVC being precaval, retrocaval, or pericaval (Fig. 3). We modified this classification by adding one more type as a SAN artery originating from middle segment of right coronary artery running medial to the right auricle (R1m) (Fig. 4). We also recorded the communication between the SAN artery and bronchial artery.

Statistical Analysis

All statistical analyses were performed by Pearson's chi-Square test using the statistical software package (SPSS 18.0 for Windows, SPSS Inc, Chicago, IL, USA). A *p* value of less than 0.05 was considered to be statistically significant.

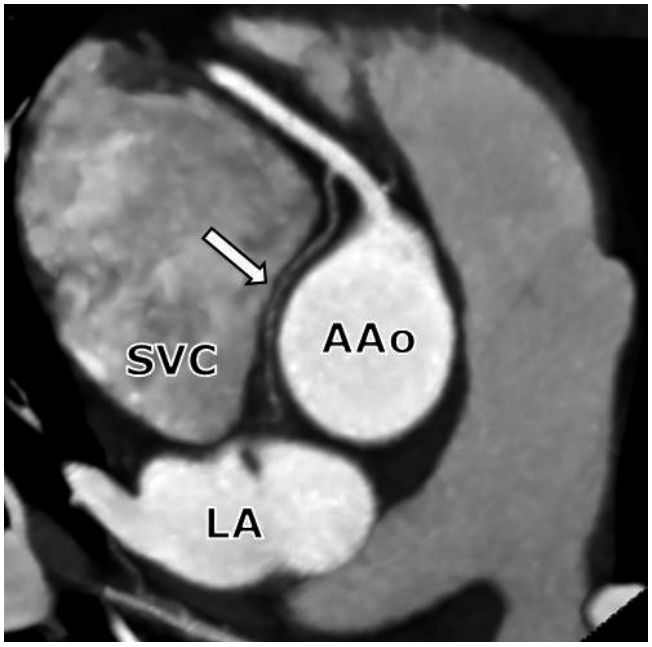

Fig. 1. R1 subtype SAN artery (white arrow) arising from RCA is seen in axial MIP view. AAo = ascending aorta, LA = left arium, SVC = superior vena cava, SAN = sinoatrial node, RCA = right coronary artery, R1 = medial to the right auricle, MIP = maximum ittensity projection

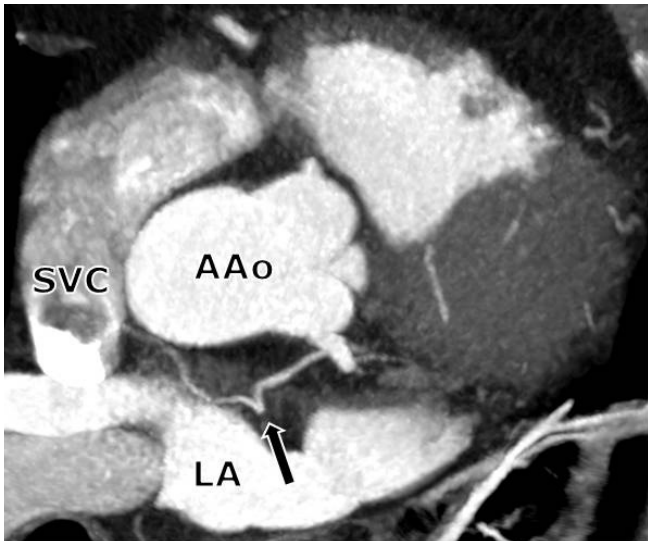

Fig. 2. L1 subtype SAN artery (black arrow) arising from LCX is seen in axial MIP view. AAo = ascending aorta, LA = left arium, SVC = superior vena cava, SAN = sinoatrial node, MIP = maximum ittensity projection, LCX = left circumflex

RESULTS

The SAN artery was visualized in 496 of 500 cases. The SAN was supplied by a single artery in 478 (96.4%) cases and by 2 arteries in 18 (3.6%) cases. A single SAN artery arose from the RCA in 265 (53.4%) cases and from the LCX artery in 213 (43.0%) cases. The SAN was supplied by 2 branches, each arising from RCA and LCX in 18 (3.6%) cases. Communication between RCA originating SAN artery and bronchial artery was observed in 3 (0.6%) cases. These 3 SAN arteries from the RCA were all classified as the R1 subtype.

When all SAN arteries were evaluated individually, the total number of SAN arteries was 514 (Table 1). The termination types in the 514 SAN arteries were precaval in 105 (20.4%), retrocaval in 246 (47.9%) and pericaval in 163 (31.7%). There was no statistically significant relationship between the origin of the SAN artery and the course of the terminal segment (p = 0.31). The retrocaval type was the most frequent in all SAN artery subtypes.

The single R1 retrocaval type, which was observed in 132 (26.6%) of 496 patients, was the most frequent type. In addition, the single R1 retrocaval type was observed most frequently when the patients were grouped by gender.

The S-shaped SAN artery which is considered to be a variant of the SAN artery arising from LCX was found in 10 cases (2.0% of all patients and 4.3% of all individual SAN arteries arising from the LCX artery) (Fig. 5). The S-shaped SAN artery was a single SAN artery in eight cases and a component of dual SAN arteries in two cases.

DISCUSSION

Various frequencies of the origin of the SAN artery were reported in several related articles (6-18, 21-24). Most of these studies (7-18, 21-23) reported that the SAN artery predominantly originates from the RCA (50-85%), followed by the LCX (10-45%) and tour results agree with these reports. Only one study (24) reported that the SAN artery predominantly originates from the LCX (49.1%), followed by the RCA (48.1%). Although the SAN artery arising from the trunk of the left coronary artery or right sinus valsalva was reported in several studies (6, 11, 13, 23), we have not encountered a SAN artery arising from them. The SAN artery arising from the bronchial artery was reported in 1.2% and 2.0% of cases in 2 separate studies (17, 23). Communication between the bronchial artery and SAN artery from the right coronary artery was encountered in 3 of 496 cases (0.6%) in our study. However, MDCT could not evaluate the direction of blood flow in these communications. Furthermore, bronchial to coronary artery fistula or communication can cause myocardial ischemia induced by a coronary steal phenomenon (27, 28). Thus, we could not determine whether these bronchial arteries

Korean Journal of Radiology
KJR

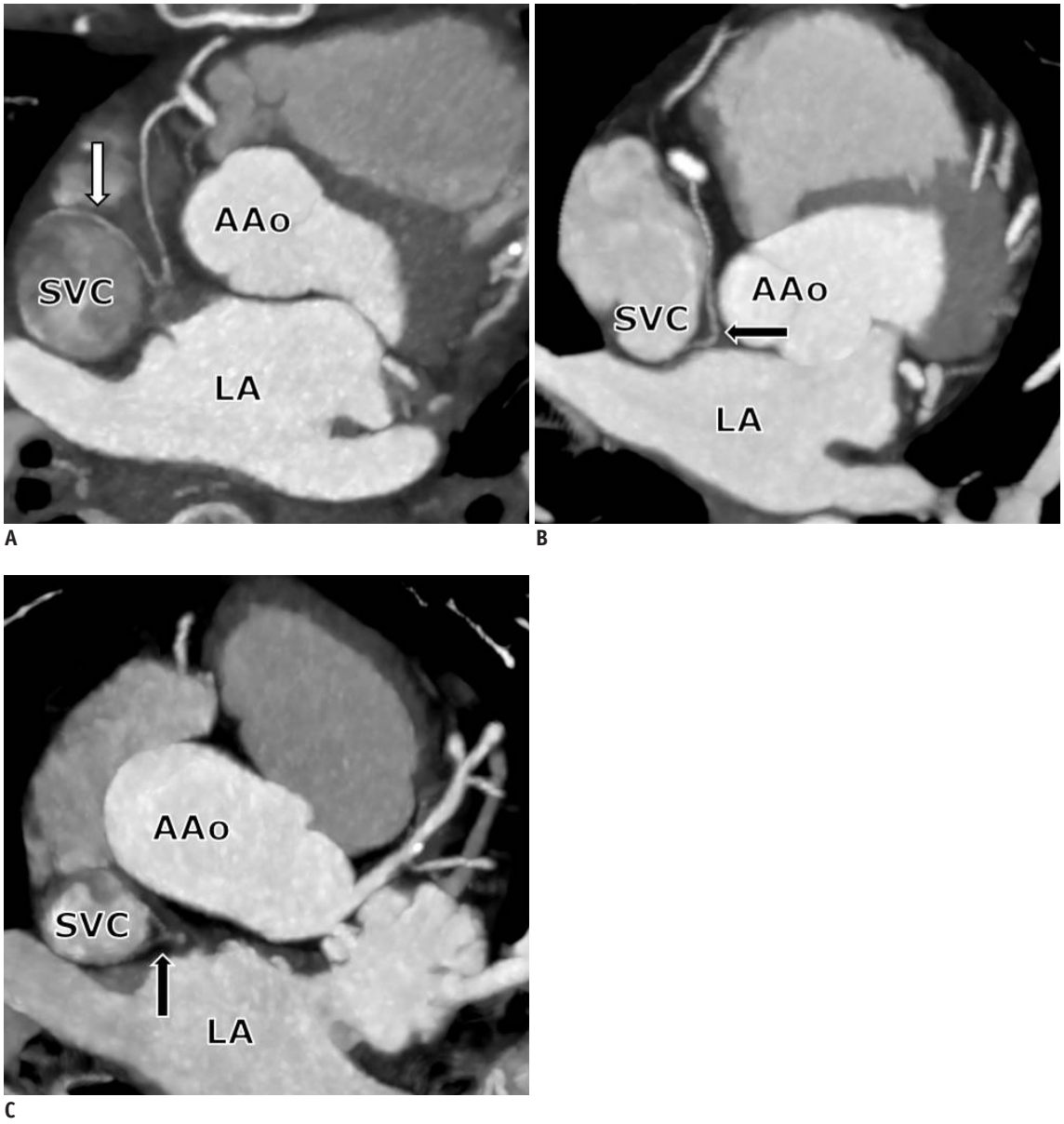

Fig. 3. MIP images show SAN artery subtypes according to course of terminal segment around SVC.
A. Precaval (white arrow). **B.** Retrocaval (black arrow). **C.** Pericaval (black arrow). AAo = ascending aorta, LA = left arium, MIP = maximum ittensity projection, SAN = sinoatrial node, SVC = superior vena cava

supplied SAN or not, and there was no single bronchial artery supplying SAN. In reference to the dual SAN artery, the results presented are consistent with those obtained by several authors (12, 17, 21-23) and less frequent than those obtained by other authors (7, 14-16, 24). For the component of dual SAN artery, our results compare well with previous reports (7, 10, 12, 14-17, 21-23), in that the dual SAN artery mostly originates from the RCA and the LCX. We found that only dual SAN arteries consist of separate branches from the RCA and LCX in 18 out of 496 cases. Triple SAN, which was reported as 2.0% and 3.8% in 2 separate studies (16, 17), was not identified in any of our cases.

In several studies (12, 21-24), the course of the terminal segment of SAN artery around SVC was classified as precaval, retrocaval, or pericaval. Among the 3 types of termination, the retrocaval and pericaval type can be surgically injured during superior trans-septal incisions (21, 29-31). Most of the previous studies reported that the retrocaval type is the most frequent (47.5-64.7%), followed by the precaval-type (25.2-42.6%) or the pericaval-type (5.9-40%). Only one study (12) reported that the precaval type is the most frequent type (58%) of termination. Similar to most of former studies, we have found mostly retrocaval-type

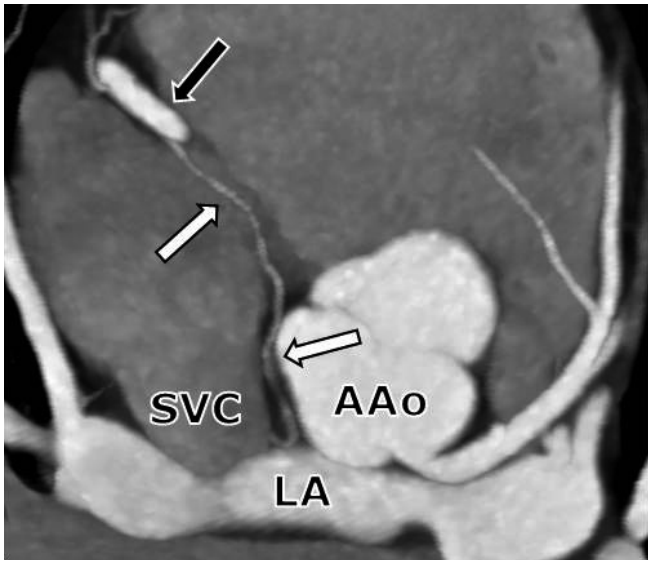

Fig. 4. R1m subtype SAN artery (white arrows) arising from middle segment of RCA (black arrow). AAo = ascending aorta, LA = left arium, SAN = sinoatrial node, SVC = superior vena cava, RCA = right coronary artery, R1m = originated from middle segment of right coronary artery and run medial to right auricle

termination.

When all arteries are evaluated individually except for the R1m subtype (Table 1), the most frequent subtype in our study was R1 (54.5%), followed by L1 (33.3%). Two previous studies using same classification also found that R1 is the most frequent subtype (46-54.4%), followed by L1 (21.5-24%). They also found rare SAN arteries which run on the posterior surface of the right (R2 subtype, 1.2-4%) or left atrium (L3 subtype, 0.4-4%). However, we have not encountered any case of R2 or L3 type. Rarity of these subtypes may explain our observation.

The R1m subtype is part of the R1 subtype by definition used in Ortale et al. (17) and Ozturk et al. (23). Ortale et al. (17) reported that the longest distance between the RCA ostium and the origin of the SAN artery from the RCA was 48.6 mm. Ozturk et al. (23) reported the longest distance between the RCA ostium and origin of the SAN artery from the RCA to be 62 mm. The R1m subtype might be included in these studies. As such, R1m may not be a

Table 1. Types of SAN Arteries and Their Frequencies with Individual Evaluation

Origin of SAN Artery	RCA (%)			LCX (%)		
Subtype	R1	R1m	R2	L1	L2	L3
Precaval	50 (9.7)	0 (0.0)	0 (0.0)	46 (8.9)	9 (1.8)	0 (0.0)
Retrocaval	134 (26.1)	3 (0.6)	0 (0.0)	75 (14.6)	34 (6.6)	0 (0.0)
Pericaval	96 (18.7)	0 (0.0)	0 (0.0)	50 (9.7)	17 (3.3)	0 (0.0)
Total	280 (54.5)	3 (0.6)	0 (0.0)	171 (33.3)	60 (11.7)	0 (0.0)

Note.— SAN = sinoatrial node, RCA = right coronary artery, LCX = left circumflex, R1 = medial to right auricle, R1m = originated from middle segment of right coronary artery and run medial to right auricle, R2 = on posterior surface of right atrium, L1 = medial to left auricle, L2 = posterior to left auricle, L3 = on posterior surface of left atrium

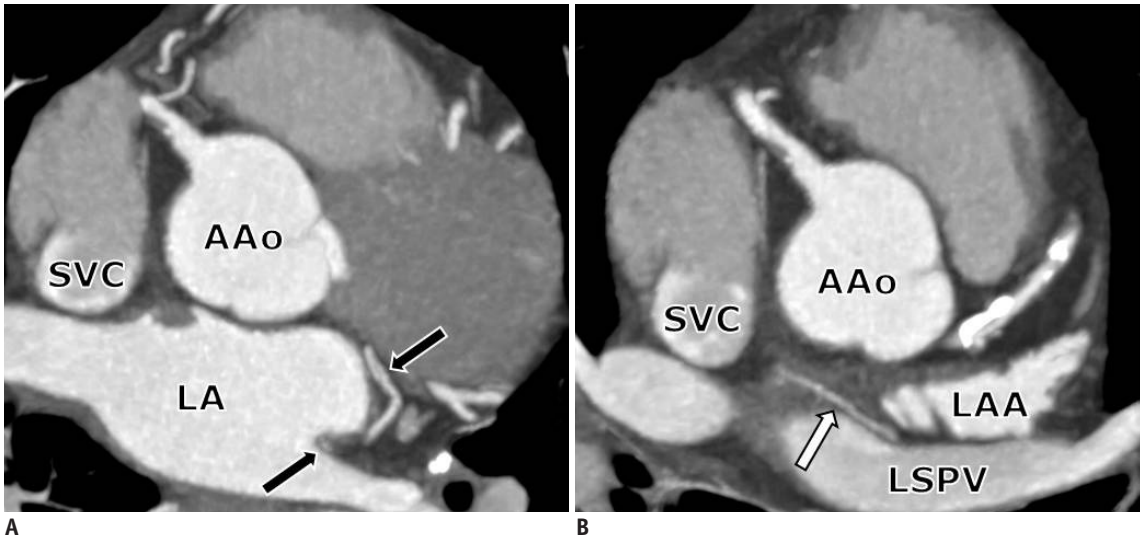

A B

Fig. 5. S-shaped SAN artery (black and white arrows) arising from LCX and running between left superior pulmonary vein and left atrial auricular is seen in MIP images (A, B). AAo = ascending aorta, SAN = sinoatrial node, SVC = superior vena cava, LAA = left atrial appendage, LCX = left circumflex, LSPV = left superior pulmonary vein, MIP = maximum ittensity projection

Korean Journal of Radiology
KJR

unique subtype of the Korean population. However, these reports did not mention whether the longest distance was associated with the R1 or R2 subtype. Further study with exact measurements of distance between the RCA ostium and origin of the SAN artery in each subtype is warranted.

The S-shaped SAN artery is a well-known anatomical variation of the SAN artery arising from the proximal LCX. The S-shape SAN artery arises from the posterolateral part of the LCX below, or behind the left auricle, and runs posteriorly between the left atrial appendage and the ostium of the left superior pulmonary vein, and then anteriorly close to the anterior wall of the left atrium (22). Because the S-shape SAN artery runs close to the left atrial wall, a lack of awareness about this variation can cause vessel injury during a surgical intervention or during a catheter-based ablation of the left atrium. In previous studies, the frequency of the S-shaped SAN artery is reported to be between 5.9% and 20.3% (17, 21-24, 32). We (1.9% of all cases) encountered the S-shaped SAN artery less frequently than previous studies had encountered this anatomic variation.

In conclusion, types and frequencies of variations in the SAN artery in the Korean population are largely similar to previous studies, although there are some differences. This study can provide basic data on variations of the SAN artery in the Korean population.

REFERENCES

1. Ando' G, Gaspardone A, Proietti I. Acute thrombosis of the sinus node artery: arrhythmological implications. *Heart* 2003;89:E5
2. de Groot NM, Schalij MJ. The relationship between sinus node dysfunction, bradycardia-mediated atrial remodelling, and post-operative atrial flutter in patients with congenital heart defects. *Eur Heart J* 2006;27:2036-2037
3. Angelini P. Normal and anomalous coronary arteries: definitions and classification. *Am Heart J* 1989;117:418-434
4. Baltaxe HA, Wixson D. The incidence of congenital anomalies of the coronary arteries in the adult population. *Radiology* 1977;122:47-52
5. Datta J, White CS, Gilkeson RC, Meyer CA, Kansal S, Jani ML, et al. Anomalous coronary arteries in adults: depiction at multi-detector row CT angiography. *Radiology* 2005;235:812-818
6. Campbell JS. Stereoscopic radiography of the coronary system. *Quart J Med* 1929;22:247-268
7. Vieweg WV, Alpert JS, Hagan AD. Origin of the sinoatrial node and atrioventricular node arteries in right, mixed, and left inferior emphasis systems. *Cathet Cardiovasc Diagn* 1975;1:361-373
8. Okmen AS, Okmen E. Sinoatrial node artery arising from posterolateral branch of right coronary artery: definition by screening consecutive 1500 coronary angiographies. *Anadolu Kardiyol Derg* 2009;9:481-485
9. James TN. Anatomy of the human sinus node. *Anat Rec* 1961;141:109-139
10. Romhilt DW, Hackel DB, Estes EH Jr. Origin of blood supply to sinoauricular and atrioventricular node. *Am Heart J* 1968;75:279-280
11. Bokeriya LA, Mikhailin SI, Revishvili AS. Anatomical variants of sinoatrial and atrioventricular node arteries. *Cor Vasa* 1984;26:220-228
12. Busquet J, Fontan F, Anderson RH, Ho SY, Davies MJ. The surgical significance of the atrial branches of the coronary arteries. *Int J Cardiol* 1984;6:223-236
13. Caetano AG, Lopes AC, DiDio LJ, Prates JC. [Critical analysis of the clinical and surgical importance of the variations in the origin of the sinoatrial node artery of the human heart]. *Rev Assoc Med Bras* 1995;41:94-102
14. Sow ML, Ndoye JM, Lô EA. The artery of the sinuatrial node: anatomic considerations based on 45 injection-dissections of the heart. *Surg Radiol Anat* 1996;18:103-109
15. Futami C, Tanuma K, Tanuma Y, Saito T. The arterial blood supply of the conducting system in normal human hearts. *Surg Radiol Anat* 2003;25:42-49
16. Kawashima T, Sasaki H. The morphological significance of the human sinuatrial nodal branch (artery). *Heart Vessels* 2003;18:213-219
17. Ortale JR, Paganoti Cde F, Marchiori GF. Anatomical variations in the human sinuatrial nodal artery. *Clinics (Sao Paulo)* 2006;61:551-558
18. Hadziselimović H. Vascularization of the conducting system in the human heart. *Acta Anat (Basel)* 1978;102:105-110
19. Park BJ, Sung DJ, Kim MJ, Cho SB, Kim YH, Chung KB, et al. The incidence and anatomy of accessory pudendal arteries as depicted on multidetector-row CT angiography: clinical implications of preoperative evaluation for laparoscopic and robot-assisted radical prostatectomy. *Korean J Radiol* 2009;10:587-595
20. Kumar S, Neyaz Z, Gupta A. The utility of 64 channel multidetector CT angiography for evaluating the renal vascular anatomy and possible variations: a pictorial essay. *Korean J Radiol* 2010;11:346-354
21. Saremi F, Abolhoda A, Ashikyan O, Milliken JC, Narula J, Gurudevan SV, et al. Arterial supply to sinuatrial and atrioventricular nodes: imaging with multidetector CT. *Radiology* 2008;246:99-107; discussion 108-109
22. Saremi F, Channual S, Abolhoda A, Gurudevan SV, Narula J, Milliken JC. MDCT of the S-shaped sinoatrial node artery. *AJR Am J Roentgenol* 2008;190:1569-1575
23. Ozturk E, Saglam M, Bozlar U, Kemal Sivrioglu A, Karaman B, Onat L, et al. Arterial supply of the sinoatrial node: a CT coronary angiographic study. *Int J Cardiovasc Imaging* 2011;27:619-627

24. Zhang LJ, Wang YZ, Huang W, Chen P, Zhou CS, Lu GM. Anatomical investigation of the sinus node artery using dual-source computed tomography. *Circ J* 2008;72:1615-1620
25. Buss DD, Hyde DM, Steffey EP. Coronary collateral development in the rhesus monkey (Macaca mulatta). *Basic Res Cardiol* 1983;78:510-517
26. Petronio AS, Baglini R, Limbruno U, Mengozzi G, Amoroso G, Cantarelli A, et al. Coronary collateral circulation behaviour and myocardial viability in chronic total occlusion treated with coronary angioplasty. *Eur Heart J* 1998;19:1681-1687
27. Lee CM, Leung TK, Wang HJ, Lee WH, Shen LK, Chen YY. Identification of a coronary-to-bronchial-artery communication with MDCT shows the diagnostic potential of this new technology: case report and review. *J Thorac Imaging* 2007;22:274-276
28. Peynircioglu B, Ergun O, Hazirolan T, Cil BE, Aytemir K. Bronchial to coronary artery fistulas: an important sign of silent coronary artery disease and potential complication during bronchial artery embolization. *Acta Radiol* 2007;48:171-172
29. Gaudino M, Alessandrini F, Glieca F, Martinelli L, Santarelli P, Bruno P, et al. Conventional left atrial versus superior septal approach for mitral valve replacement. *Ann Thorac Surg* 1997;63:1123-1127
30. Misawa Y, Fuse K, Kawahito K, Saito T, Konishi H. Conduction disturbances after superior septal approach for mitral valve repair. *Ann Thorac Surg* 1999;68:1262-1264; discussion 1264-1265
31. Lanciego C, Rodriguez M, Rodriguez A, Carbonell MA, García LG. Permanent pacemaker-induced superior vena cava syndrome: successful treatment by endovascular stent. *Cardiovasc Intervent Radiol* 2003;26:576-579
32. Raff GL, Gallagher MJ, O'Neill WW, Goldstein JA. Diagnostic accuracy of noninvasive coronary angiography using 64-slice spiral computed tomography. *J Am Coll Cardiol* 2005;46:552-557